

Improving efficiency of n-i-p perovskite solar cells enabled by 3-carboxyphenylboronic acid additive

Bin-Jie Li(李斌杰), Jia-Wen Li(李嘉文), Gen-Jie Yang(杨根杰), Meng-Ge Wu(吴梦鸽), and Jun-Sheng Yu(于军胜)
Citation: Chin. Phys. B, 2023, 32 (**10**): 107801. DOI: 10.1088/1674-1056/ace1d8
Journal homepage: http://cpb.iphy.ac.cn; http://iopscience.iop.org/cpb

What follows is a list of articles you may be interested in

Exciton luminescence and many-body effect of monolayer WS_2 at room temperature

Jian-Min Wu(吴建民), Li-Hui Li(黎立辉), Wei-Hao Zheng(郑玮豪), Bi-Yuan Zheng(郑弼元), Zhe-Yuan Xu(徐哲元), Xue-Hong Zhang(张学红), Chen-Guang Zhu(朱晨光), Kun Wu(吴琨), Chi Zhang(张弛), Ying Jiang(蒋英),Xiao-Li Zhu(朱小莉), and Xiu-Juan Zhuang(庄秀娟)
Chin. Phys. B, 2022, 31 (**5**): 057803. DOI: 10.1088/1674-1056/ac380c

Improving the performance of a GaAs nanowire photodetector using surface plasmon polaritons

Xiaotian Zhu(朱笑天), Bingheng Meng(孟兵恒), Dengkui Wang(王登魁), Xue Chen(陈雪), Lei Liao(廖蕾), Mingming Jiang(姜明明), and Zhipeng Wei(魏志鹏)
Chin. Phys. B, 2022, 31 (**4**): 047801. DOI: 10.1088/1674-1056/ac1e15

Enhancing the photo-luminescence stability of $CH_3NH_3PbI_3$ film with ionic liquids

Weifeng Ma(马威峰), Chunjie Ding(丁春杰), Nasrullah Wazir, Xianshuang Wang(王宪双), Denan Kong(孔德男), An Li(李安), Bingsuo Zou(邹炳锁), and Ruibin Liu(刘瑞斌)
Chin. Phys. B, 2022, 31 (**3**): 037802. DOI: 10.1088/1674-1056/ac3067

Conductance and dielectric properties of hydrogen and hydroxyl passivated SiCNWs

Wan-Duo Ma(马婉铎), Ya-Lin Li(李亚林), Pei Gong(龚裴), Ya-Hui Jia(贾亚辉), and Xiao-Yong Fang(房晓勇)
Chin. Phys. B, 2021, 30 (**10**): 107801. DOI: 10.1088/1674-1056/abf130

Studies on the polycrystalline silicon/SiO_2 stack as front surface field for IBC solar cells by two-dimensional simulations

Shuai Jiang(姜帅), Rui Jia(贾锐), Ke Tao(陶科), Caixia Hou(侯彩霞), Hengchao Sun(孙恒超), Zhiyong Yu(于志泳), Yongtao Li(李勇滔)
Chin. Phys. B, 2017, 26 (**8**): 087802. DOI: 10.1088/1674-1056/26/8/087802

Improving efficiency of n–i–p perovskite solar cells enabled by 3-carboxyphenylboronic acid additive

Bin-Jie Li(李斌杰), Jia-Wen Li(李嘉文), Gen-Jie Yang(杨根杰), Meng-Ge Wu(吴梦鸽), and Jun-Sheng Yu(于军胜)†

State Key Laboratory of Electronic Thin Films and Integrated Devices, School of Optoelectronic Science and Engineering, University of Electronic Science and Technology of China (UESTC), Chengdu 610054, *China*

(Received 27 April 2023; revised manuscript received 15 June 2023; accepted manuscript online 27 June 2023)

In the past period of time, perovskite solar cells have gained tremendous developments in improving photovoltaic performance, but they still face severe challenges. Defects in perovskite layers, especially at grain boundaries, severely limit the stabilization and efficiency of solar cells. In this work, we adopt 3-carboxyphenylboronic acid (CPBA) for modifying defects in perovskite thin films. Through the interaction among the carboxyl group, boronic acid and lead ions in the perovskite film, the crystallization effect of the perovskite molecular is greatly optimized. Moreover, the film defects are spontaneously passivated and the band gap is reduced, increasing the open circuit voltage and fill factor. Therefore, power conversion efficiency has been increased from 17.25% to 20.20%. This discovery provides a potential strategy for passivating the trap states in perovskite and enhancing the properties of devices.

Keywords: passivation, defects, 3-carboxyphenylboronic acid, perovskite solar cells

PACS: 78.56.–a, 88.40.hj, 73.61.–r, 61.72.–y **DOI:** 10.1088/1674-1056/ace1d8

1. Introduction

Perovskite solar cells (PSCs) have become a hot research topic in the field of photovoltaics due to their strong photoelectric conversion performance,[1,2] tunable band gap,[3,4] simple structure,[5] outstanding flexibility,[6] and mature manufacturing process.[7] Since their debut in 2009, PSCs have seen explosive growth in PCE, from 3.8% to 25.7%.[8–11] The perovskite layer is the core part of PSCs, and the quality of its film has an essential effect on the properties and stability of perovskite devices. Nonradiative recombination induced by traps on the surface of perovskite grains and junction of grains is the major obstacle to achieving high PCE and the long-term stability of PSCs.[12] Instead, a uniform morphology can reduce shunting paths, expand light collection, and help improve the quality of adjacent charge transport layers.[13,14] Obtaining dense, large-grain-size perovskite films has become the focus of research in various research groups. The morphology optimization of perovskite films,[15] such as film coverage, roughness, grain size, and grain boundaries, has been considered as important factors to achieve high extremely efficiency.

At present, additive engineering is a useful method for controlling the quality of the resulting perovskite layer thin films. For example, Grätzel *et al*. used ammonium phosphonate as an additive to optimize the surface of perovskite films,[16] ammonium phosphonate acts as a crosslinker between adjacent perovskite grains through strong hydrogen bonding. Huang *et al*. used 3-(decyldimethylammonium)-propane sulfonic acid inner salt (DPSI) as an additive.[17] They proposed that the coordination of the sulfonic acid groups of DPSI to perovskite molecules were achieved by donating their lone pairs of electrons to the empty orbitals of lead ions. Park *et al*. added (3-mercaptopropyl) trimethoxysilane (MPTS) as an additive to the PbI_2 solution to fill the surface defects, thereby significantly improving thermal and moisture stability.[18] By summarising the previous studies, we can find that these additives were added to the perovskite by doping, and the functional groups of the additives were connected with the perovskite molecules through hydrogen bonding or coordination to achieve the purpose of modification.

In this work, we improved the PCE of the devices for the first time by modifying perovskite films by using 3-carboxyphenylboronic acid (CPBA) as an additive. The carboxyl and boronic acid groups interact with uncoordinated iodide or lead ions in perovskites, which passivate the trap states at grain boundaries and inhibit the migration of ions, resulting in tight intermolecular connections in perovskites. After passivation treatment with an appropriate concentration of CPBA, the band gap became smaller and the open circuit voltage and fill factor increased. Moreover, the PCE increased from 17.25% in the control group to 20.20% in the experimental group. At the same time, other performances of the experimental group were also improved more or less. Our study provides a potential strategy for passivating perovskite thin films and enhancing the PCE of PSCs.

†Corresponding author. E-mail: jsyu@uestc.edu.cn

© 2023 Chinese Physical Society and IOP Publishing Ltd

2. Experimental details

2.1. Materials and solvent

Isopropyl alcohol (IPA 99.5%), N,N-dimethylformamide (DMF, 99.8%), dimethyl sulfoxide (DMSO, 99%), 4-tert-butylpyridine (tBP, 96%), chlorobenzene (CB, 99.5%), Li-TFSI (99.95%), FK 209, and acetone (AC, 99.5%) were obtained from Sigma-Aldrich Corporation. 2,2′,7,7′-tetrakis[N,N-di(4-methoxyphenyl)amino]-9,9′-spirobifluorene (spiro-OMeTAD) and indium tin oxide (ITO) substrates were obtained from Liaoning Youxuan New Energy Technology Corporation. Formamidinium iodide (FAI), methylammonium bromide (MABr), methylammonium chloride (MACl), lead iodide (PbI_2), and 3-carboxyphenylboronic acid (CPBA) were obtained from Xi'an Polymer Light Technology Corporation. And all other chemical materials were used as obtained with no need for more refined processing.

2.2. Thin-film and solar cell fabrication

ITO/SnO_2/perovskite/spiro-OMeTAD/MoO_3/Ag structure is employed for the devices in this work. Clean the ITO substrates with dishwashing liquid, AC, deionized (DI) water, and IPA for fifteen minutes, respectively. After air-drying in the oven, the ITO substrates were irradiated under UV ozone for 20 minutes. Diluted SnO_2 colloidal solution (2.67 vol%) was spin-coated at 3500 rpm for 35 seconds and annealed at 150 °C for 25 minutes. Next, the substrates were put into a glovebox (with nitrogen both oxygen and water below 2.0 ppm). For functional layer preparation, 40 μL of PbI_2 precursor solution (950 μL of DMF, 50 μL of DMSO, and 599.3 mg of PbI_2) was spin-coated at 1800 rpm for 36 seconds, and annealed at 70 °C for 1 minute. 40 μL of ammonium salt solution (60 mg of FAI, 6 mg of MACl, 6 mg of MABr, CPBA of different masses, and 1 mL of IPA) was spin-coated at 2200 rpm for 35 seconds, followed by anneal at 160 °C for 18 minutes, the humidity is controlled at 30%. When the temperature of the substrates dropped to about the same as the surrounding environment, the spiro-OMeTAD solution (1 mL of CB, 72 mg of spiro-OMeTAD, 28 μL of tBP, 18 μL of Li-TFSI (520 mg·mL^{-1} of AN), and 2 mg of FK 209) was spin-coated at 4000 rpm for 35 seconds without annealing. At last, MoO_3 (8 nm) and Ag (100 nm) were vapor-deposited at a pressure of 0.003 Pa.

2.3. Characterization techniques

A xenon lamp (HSX-F300) was used as the light source to simulate the light power of standard sunlight (100 mW·cm^{-2}), while silicon solar cells were used for the calibration of light intensity. Voltametric specificity (J–V) curves tests were executed by semiconductor parameter analyzer (Keithley 4200). External quantum efficiency (EQE) spectra curves tests were executed by solar quantum effect test system. The microstructure tests of the film surface were executed by scanning electron microscopy (SEM) and atomic force microscopy (AFM). The crystallization situation tests were executed by x-ray diffraction (XRD) and x-ray photoelectron spectroscopy (XPS) with a source of monochromatic Al-Ka. The energy levels of perovskites tests were executed by ultraviolet-vis (UV-Vis) absorption and UV photoelectron spectroscopy (UPS). Carrier excitation and excitation properties tests were executed by steady-state photoluminescence (PL). Carrier decay lifespan tests were executed by time-resolved PL (TRPL). These tests were executed at indoor ambient temperature conditions.

3. Results and discussion

As shown in Fig. 1(a), preparation of perovskite films using a two-step method, and CPBA was added as an additive to the precursors of FAI, MACl, and MABr in the second step. In order to obtain the optimal doping ratio, we added different amounts of CPBA to the precursor solution and the device properties are shown in Table 1. Based on PCE, the concentration of CPBA was optimized to 0.1 mg/mL. Figures 1(b) and S1 depicts the J–V data of PSCs with several doping concentrations of CPBA. The open-circuit voltage (V_{OC}) of the control group was 1.05 V, the short-circuit current density (J_{SC}) was 23.13 mA·cm^{-2}, the fill factor (FF) was 71.00%, and the PCE was 17.25%. The V_{OC} of devices with CPBA was 1.09 V, the J_{SC} was 24.71 mA·cm^{-2}, the FF was 75.14%, and the devices achieved a higher PCE of 20.20%. Compared with the control devices, the PCE is increased by 17.10%. When the concentration is too high, the device performance decreases. It can be seen from the comparison that the improvement of properties was attributed to the improvement of V_{OC}, J_{SC}, and FF. In addition, EQE spectrum of the device is shown in Fig. 1(c). The spectrum shapes of the cells show the similar trend in the wavelength (λ) range between 300 nm and 850 nm, meanwhile the EQE spectrum of the cells modified with the optimal concentration of CPBA show an overall enhancement. The integrated J_{SC} values estimated based on the EQE spectrum shapes were 22.34 mA·cm^{-2} and 23.94 mA·cm^{-2} for the control and experimental groups, correspondingly.

Table 1. Performance parameters of PSCs with CPBA concentrations.

Sample	V_{OC} (V)	J_{SC} (mA/cm^2)	FF (%)	PCE (%)
Control	1.05±0.01	23.13±0.36	71.00±1.95	17.25±0.85
0.05 mg/mL	1.03±0.01	24.25±0.18	72.42±1.19	18.12±0.36
0.1 mg/mL	1.09±0.01	24.71±0.08	75.14±1.66	20.20±0.55
0.5 mg/mL	1.07±0.02	24.05±0.14	72.42±1.55	18.62±0.66
1 mg/mL	1.11±0.01	22.31±0.32	67.83±1.97	16.80±0.61

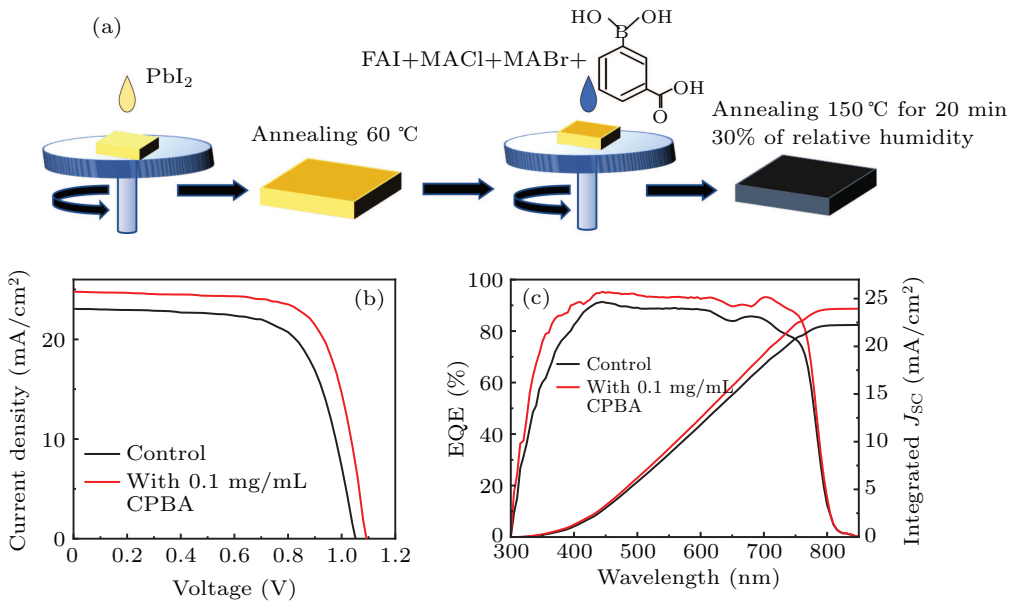


Fig. 1. (a) Flow chart of the perovskite thin films preparation, (b) *J*–*V* curves of PSC devices treated without and with CPBA under 100 mW·cm^{-2}, and (c) the corresponding EQE spectra.

To explore the change of CPBA on the surface appearance of perovskite films, the sample with a formation of ITO/SnO_2/perovskite was prepared, and we characterized the perovskite films using SEM and AFM. Figures 2(a), 2(b) and S2(a)–S2(c) show the SEM overhead photographs of the control perovskite films and the films doped with CPBA. Figure S3 shows the grain size distribution of Figs. 2(a) and 2(b). The average diameter of the crystals increases with increasing CPBA content compared to the untreated perovskite films. As can be seen in Figs. 2(a) and 2(b), the pure perovskite film has small grains and insufficient connections, and there are some small holes in the film. After being modified with CPBA, we can notice that the particles of the films get significantly larger, and the gap is smaller. However, as the doping content of CPBA changes from 0.05 mg·mL^{-1} to 1 mg·mL^{-1}, the grain uniformity decreases and more white particles occupy the grain edge compared with the control perovskite films. These white particles may be caused by too much CPBA. When the concentration of additives is low, CPBA helps perovskite film formation, compensate for defects, optimize the qualities of the film, and enhance the photovoltaic performance. When the concentration is high, although there is a certain benefit for V_{OC}, the accumulation of excess CPBA may affect the transfer of carriers and inhibit the photocurrent. Figures 2(c), 2(d) and S4(a)–S4(c) show the AFM characterization photographs of the perovskite films with no additives and the films with additives doped with several contents. The root-mean-square (RMS) value of the roughness for each film was also interpolated. It can be seen that the film with doping concentration of 0.1 mg·mL^{-1} has the lowest roughness, which is corresponded to the SEM photographs' results. Smooth and uniform perovskite thin films contribute to easier carrier diffusion and thus improved photovoltaic performance. The larger and more homogeneous crystal diameter of the hybrid perovskite films indicates defect reduction as well as nonradiative recombination centers, which are beneficial for achieving enhanced photovoltaic performance. However, excessive roughness will affect the film properties, form new non-radiative recombination centers, and reduce the photovoltaic performance.[19]

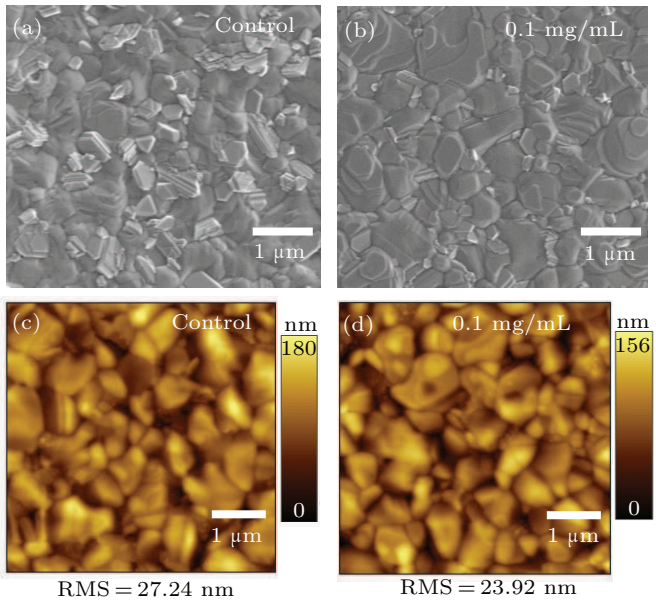


Fig. 2. (a)–(b) Top view SEM images and (c)–(d) top view AFM images of perovskite films treated without and with CPBA.

To more deeply explore the role of CPBA in perovskite, we selected 0.1 mg/mL CPBA-modified perovskite film as the experimental group and pure perovskite film as the control group. The sample with a structure of ITO/SnO_2/perovskite was prepared, and XRD and XPS experiments were carried out. As shown in Fig. 3(a), we can see that the perovskite film has strong diffraction peaks at 2θ around 14°, 28°, and 32°,

which are respectively attributed to the (110), (220), and (310) planes of the perovskite crystal.[20] The height of the diffraction peaks of XRD indicates the crystallization of the crystal. Usually, the higher the diffraction peak of XRD, the better the crystallization of the crystal, which is more conducive to transmission of carriers.[21] Compared with the films of the control group, the peaks in the experimental group appear higher and sharper in the typical cubic phase crystal orientation, and it can be assumed that CPBA compensates for the defects in the film by coordination with the perovskite molecules and promotes grain growth in the cubic phase, resulting in improved crystallinity. It also matches the images observed in the SEM. Figure S5 is the full XPS spectrum of CPBA-treated perovskite. In Fig. 3(b), we show the XPS analysis of lead on the perovskite thin films. Comparing the experimental group with the control group, it can be found that there are two obvious Pb $4f_{7/2}$ peaks and two obvious Pb $4f_{5/2}$ peaks, which indicates that the surface exists an interaction between CPBA and lead.[22] It is presumed that the boronic acid group in CPBA provides the lone pair of electrons to react with the uncoordinated lead ion, causing the lead to move in the direction of lower binding energy.

To characterize the light absorption properties as well as energy levels of devices, perovskite films were fabricated on quartz glass and tested by UV-Vis and UPS. As shown in Fig. S6(a), the experimental group can lead to larger absorption in most of the absorption region of visible light, which demonstrates that the addition of CPBA changes the absorption properties of perovskite films. The energy band gap (E_g) of the perovskite is determined according to [23]

$$(\alpha h\nu)^{1/n} = A\left(h\nu - E_g\right), \tag{1}$$

where α denotes the absorption factor, h denotes Planck's constant, ν denotes the frequency, and A is a constant. Since perovskite is a direct bandgap semiconductor, n is taken as 1/2. Figures S6(b)–S6(c) describe the tauc plots of the perovskite film.[24,25] The Fermi level is[26]

$$E_F = -\left(h\nu - E_{cut-off}\right), \tag{2}$$

where the value of $h\nu$ is 21.22 eV, which denotes the energy of the UV photons (He-α), while $E_{cut-off}$ represents the cut-off of second electrons. Figures 4(a) and 4(b) show the UPS spectra of the perovskite films, from which $E_{cut-off}$ and E_{end} can be obtained. We calculated E_Fs of −3.57 eV and −3.42 eV for the control and experimental groups, correspondingly. The valence band maximum (VBM) is equal to the difference between E_F and E_{end}. We then calculated the VBM of the control group and the experimental group to be −5.35 eV and −5.30 eV. Using VBM and E_g, we could get conduction band minima (CBM) of −3.79 eV and −3.77 eV for the control and experimental groups. Therefore, we draw Fig. 4(c) based on the above measurements and calculations. After modification by CPBA, it can be seen that the band gap width of the perovskite is reduced, which is favorable for the spectral absorption. And the test results also coincide with the EQE data.

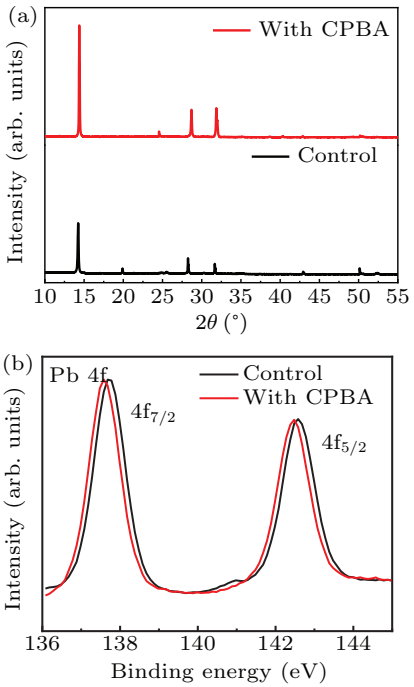


Fig. 3. (a) XRD spectra, (b) XPS spectra for Pb 4f of perovskite treated without and with CPBA.

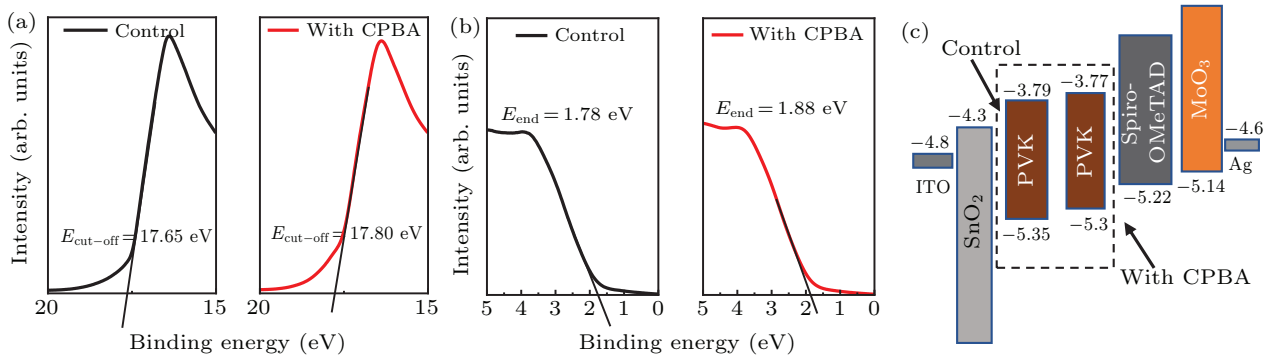


Fig. 4. (a) High binding energy UPS images and (b) low binding energy UPS images of perovskite treated without and with CPBA. (c) Energy level diagram of perovskite treated without (left) and with CPBA (right).

To explore the carrier excitation and transfer ability of the films, we prepared undoped perovskite films and perovskite films with doping concentration of 0.1 mg·mL^{-1} on quartz glass, then measured the steady-state PL and TRPL photoluminescence as shown in Fig. 5. The red shift of the PL peak in the experimental group can be found by comparing the positions of the peaks, which indicates a decrease in the energy band gap and is compatible with the previous characterization data. Compared with the control group, the PL intensity of the experimental group was significantly improved. This indicates that the films have better charge excitation ability after CPBA doping, and can effectively suppress the surface carrier recombination. To more deeply investigate the function of CPBA in the carrier diffusion motion, we performed measurements of TRPL spectra. The intensity of TRPL as a function of time can be described using a double exponential expression as follows:[27]

$$I(T) = A_1 \exp\left(-\frac{t}{\tau_1}\right) + A_2 \exp\left(-\frac{t}{\tau_2}\right), \tag{3}$$

where I denotes the normalized photoluminescence intensity, A_1 and A_2 are the coefficients of the two decay quantities, and short-lifespan τ_1 and long-lifespan τ_2 are the lifespans of the two decay quantities (Table S1). The average lifetime τ_{ave} is determined by

$$\tau_{ave} = \frac{\sum A_i \tau_i^2}{\sum A_i \tau_i}, \quad i = 1, 2. \tag{4}$$

The PL decay lifespan of the retouched film is longer than the PL decay lifespan of the ordinary film.[28] We can conclude that introducing an appropriate concentration of CPBA into perovskite can effectively suppress charge recombination, thereby enhancing the J_{SC} and PCE of PSCs.

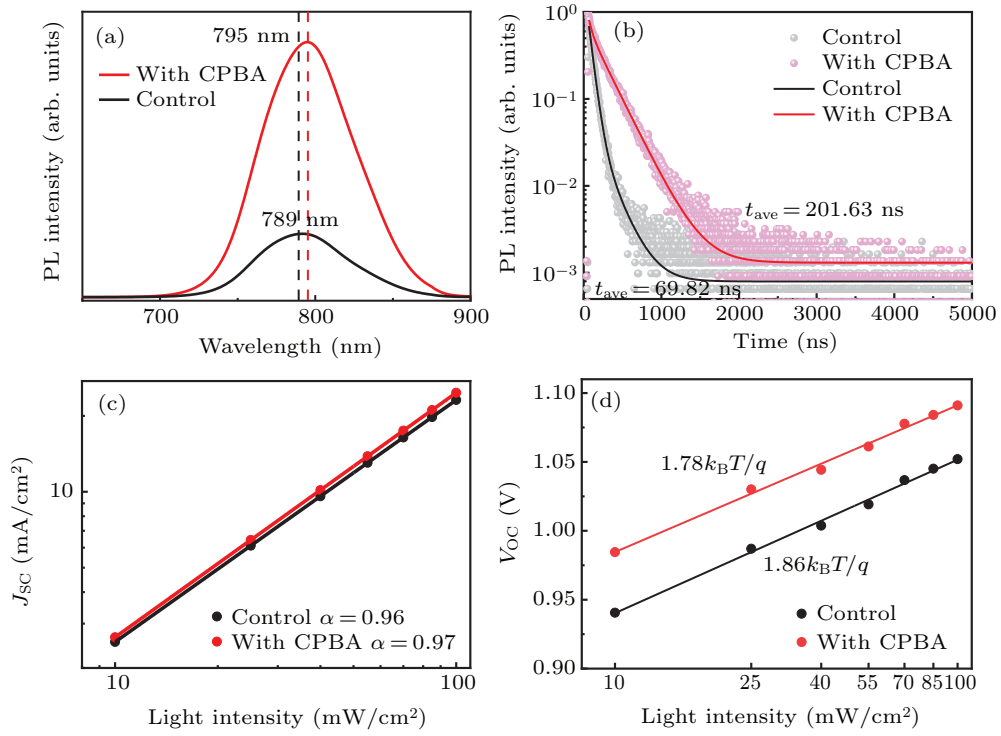


Fig. 5. (a) Steady-state PL image and (b) TRPL image of perovskite treated without and with CPBA. (c) J_{SC} and (d) V_{OC} dependence on light illumination intensity curves of PSCs treated without and with CPBA.

To investigate the carrier recombination features of the cell in depth, we performed the J_{SC} and V_{OC} measurements of the PSCs by varying the light intensity. Figure 5(c) describes the connections between J_{SC} and light intensity. The J_{SC} power law is related to light intensity as $J \propto I_\alpha$, where α denotes the incline of the curve, and devices without space charge effects show α values close to unity.[29] Here, both the control and experimental groups show a linear relationship, with an alpha value closer to 1 meaning less charge recombination. Figure 5(d) describes the connections between V_{OC} and light intensity, which are proportional to the natural logarithm of the two by a factor of $nkTq^{-1}$ (q denotes the primary charge, and T denotes the ambient temperature),[30] showing the effect of n. The less the trap in the device captures single-molecule recombination, the closer n is to 1. The n value of the control group was 1.86. However, the n value was 1.78 after modification with additives, demonstrating the reduced energy loss due to trap capture single molecule recombination. These findings correspond exactly to the data measured by PL.

At last, we tested the stability of unencapsulated devices of unmodified and doped films in the indoor environment (with 35% relative humidity and 25 °C). After one week, it can be

seen that the performance of PSCs has decreased significantly, and the modification stability of the CPBA crosslinked material has been slightly improved. Therefore, the modification of CPBA cannot improve the stability of devices effectively.

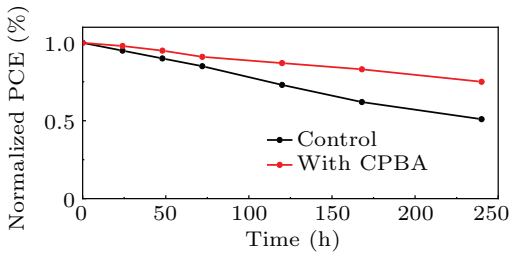


Fig. 6. Normalized PCE concerning time of PSCs treated without and with CPBA under ambient atmosphere, without encapsulation.

4. Conclusion and perspectives

In conclusion, this work demonstrates one kind of new passivation strategy using CPBA as an adulterant for the functional layer of PSCs. Combining theoretical and experimental results confirm that the strong interaction between 3-carboxyphenylboronic acid molecules and the perovskite molecules through coordination effectively decreases the thin film trap state density and inhibits the trap-assisted nonradiative recombination. Moreover, with the help of 3-carboxyphenylboronic acid passivation, the obtained perovskite films showed better morphology with increased grain size, resulting in a significant increase in PCE from 17.25% to 20.20%. Our study provides a potential strategy for passivating the trap states in perovskite and enhancing the properties of PSCs.

Acknowledgements

Project supported by the Regional Joint Fund of the National Science Foundation of China (Grant No. U21A20492), and the Sichuan Science and Technology Program (Grant Nos. 2022YFH0081, 2022YFG0012, and 2022YFG0013). This work was also sponsored by the Sichuan Province Key Laboratory of Display Science and Technology, and Qiantang Science & Technology Innovation Center.

References

[1] Kim H S, Lee C R, Im J H, Lee K B, Moehl T, Marchioro A, Moon S J, Humphry-Baker R, Yum J H, Moser J E, Grätzel M and Park N G 2012 *Sci. Rep.* **2** 591
[2] Lee M M, Teuscher J, Miyasaka T, Murakami T N and Snaith H J 2012 *Science* **338** 643
[3] Yin W J, Shi T and Yan Y 2014 *Adv. Mater.* **26** 4653
[4] De Wolf S, Holovsky J, Moon S J, Löper P, Niesen B, Ledinsky M, Haug F J, Yum J H and Ballif C 2014 *J. Phys. Chem. Lett.* **5** 1035
[5] Xing G, Mathews N, Sun S, Lim S S, Lam Y M, Grätzel M, Mhaisalkar S and Sum T C 2013 *Science* **342** 344
[6] Edri E, Kirmayer S, Cahen D and Hodes G 2013 *J. Phys. Chem. Lett.* **4** 897
[7] Stranks Samuel D, Eperon Giles E, Grancini G, Menelaou C, Alcocer Marcelo J P, Leijtens T, Herz Laura M, Petrozza A and Snaith Henry J 2013 *Science* **342** 341
[8] Kojima A, Teshima K, Shirai Y and Miyasaka T 2009 *J. Amer. Chem. Soc.* **131** 6050
[9] Min H, Lee D Y, Kim J, Kim G, Lee K S, Kim J, Paik M J, Kim Y K, Kim K S, Kim M G, Shin T J and Il Seok S 2021 *Nature* **598** 444
[10] Chen H, Ye F, Tang W, He J, Yin M, Wang Y, Xie F, Bi E, Yang X, Grätzel M and Han L 2017 *Nature* **550** 92
[11] Chiang C H, Nazeeruddin M K, Grätzel M and Wu C G 2017 *Energy Environ. Sci.* **10** 808
[12] Wolff C M, Caprioglio P, Stolterfoht M and Neher D 2019 *Adv. Mater.* **31** 1902762
[13] Zheng X, Chen B, Dai J, Fang Y, Bai Y, Lin Y, Wei H, Zeng X C and Huang J 2017 *Nat. Energy* **2** 17102
[14] Yang S, Chen S, Mosconi E, Fang Y, Xiao X, Wang C, Zhou Y, Yu Z, Zhao J, Gao Y, De Angelis F and Huang J 2019 *Science* **365** 473
[15] Tailor N K, Abdi-Jalebi M, Gupta V, Hu H, Dar M I, Li G and Satapathi S 2020 *J. Mater. Chem. A* **8** 21356
[16] Zhang F, Bi D, Pellet N, Xiao C, Li Z, Berry J J, Zakeeruddin S M, Zhu K and Grätzel M 2018 *Energy Enviro. Sci.* **11** 3480
[17] Zheng X, Deng Y, Chen B, Wei H, Xiao X, Fang Y, Lin Y, Yu Z, Liu Y, Wang Q and Huang J 2018 *Adv. Mater.* **30** 1803428
[18] Son D Y, Kim S G, Seo J Y, Lee S H, Shin H, Lee D and Park N G 2018 *J. Amer. Chem. Soc.* **140** 1358
[19] Bush K A, Rolston N, Gold-Parker A, Manzoor S, Hausele J, Yu Z J, Raiford J A, Cheacharoen R, Holman Z C, Toney M F, Dauskardt R H and Mcgehee M D 2018 *ACS Energy Lett.* **3** 1225
[20] Li N, Luo Y, Chen Z, Niu X, Zhang X, Lu J, Kumar R, Jiang J, Liu H, Guo X, Lai B, Brocks G, Chen Q, Tao S, Fenning D P and Zhou H 2020 *Joule* **4** 1743
[21] Moore D T, Sai H, Tan K W, Smilgies D M, Zhang W, Snaith H J, Wiesner U and Estroff L A 2015 *J. Amer. Chem. Soc.* **137** 2350
[22] Fu S, Zhang W, Li X, Wan L, Wu Y, Chen L, Liu X and Fang J 2020 *ACS Energy Lett.* **5** 676
[23] Zhang J, Bai D, Jin Z, Bian H, Wang K, Sun J, Wang Q and Liu S 2018 *Adv. Energy Mater.* **8** 1703246
[24] Prochowicz D, Tavakoli M M, Kalam A, Chavan R D, Trivedi S, Kumar M and Yadav P 2019 *J. Mater. Chem. A* **7** 8218
[25] Zhang F, Silver S H, Noel N K, Ullrich F, Rand B P and Kahn A 2020 *Adv. Energy Mater.* **10** 1903252
[26] Azmi R, Ugur E, Seitkhan A, *et al.* 2022 *Science* **376** 73
[27] Stolterfoht M, Wolff C M, Amir Y, Paulke A, Perdigón-Toro L, Caprioglio P and Neher D 2017 *Energy Enviro. Sci.* **10** 1530
[28] Bisquert J, Zaban A, Greenshtein M and Mora-Seró I 2004 *J. Amer. Chem. Soc.* **126** 13550
[29] Kim M, Jeong J, Lu H, *et al.* 2022 *Science* **375** 302
[30] Singh T and Miyasaka T 2018 *Adv. Energy Mater.* **8** 1700677